JTEIN: Jurnal Teknik Elektro Indonesia, Vol. 7, No. 2, pp. 206-219, 2026
e-ISSN 2723-0589

Modeling Adaptive Interference Management in Ultra-Dense Networks Assisted by Reconfigurable Intelligent Surfaces Using Dynamic Soft-FFR and Clustering

Alisha Gita Gumilang[1]*, Moh Wahyu Aminullah[1], Thriska Dewi Umi Rasyda[1], M. Rayhan Al-Fiansha[1], and Ate Nurjana[1]

[1] Department of electrical Engineering, Faculty of Engineering, Universitas Tridinanti, Palembang, Indonesia

*Corresponding Author email : alisha@univ-tridinanti.ac.id

Abstract

Ultra-Dense Networks (UDN) and Reconfigurable Intelligent Surfaces (RIS) have emerged as two pivotal technologies for meeting the growing demand for network capacity and service quality. UDN boosts capacity by densely deploying femtocells, whereas RIS broadens coverage by relaying obstructed signals toward the receiver. However, the dense femtocell deployment introduces co-tier and cross-tier interference, and the reflective nature of RIS aggravates this problem, since interfering signals are likewise steered toward the receiver. To overcome this, the present study proposes an adaptive interference management scheme that combines dynamic clustering and Soft Fractional Frequency Reuse (Soft-FFR) within a RIS-assisted UDN. Clustering suppresses co-tier interference, while re-clustering and channel allocation are triggered by the network state, namely the estimated SINR and service zone of each femtocell. Four system models, the baseline, Dynamic Clustering, Dynamic Soft-FFR, and the proposed integration were simulated on a three-macrocell network with up to 330 femtocells. The proposed method achieves the best overall performance among the evaluated schemes. Compared with the baseline, the SINR CDF at 20 dB falls from 64% to 43% and the throughput CDF at 70 Mbps decreases from 84% to 62%, indicating that a substantially larger proportion of users attain high SINR and throughput. The spectral efficiency at 330 HeNBs increases from 5.9 to 6.9 bit/s/Hz, and the bit error rate is reduced from about 0.13 to 0.05. These results confirm that adaptively integrating Dynamic Clustering and Soft-FFR effectively suppresses both co-tier and cross-tier interference, thereby improving the reliability and spectral efficiency of dense RIS-assisted UDNs.

Keywords: Interference Management; RIS; Ultra Dense Network; Clustering; Soft Fractional Frequency Reuse

1. Introduction

The increasing use of mobile broadband services has led to a massive surge in wireless data traffic, making the need for high network capacity a major challenge in the development of 5G and next-generation communication systems [1],[2]. To address this challenge, Ultra-Dense Networks (UDN) are emerging as an effective technology for increasing capacity through the efficient utilization of network resources [3]. Through network densification specifically by deploying a large number of small cells, particularly femtocells or Home eNodeBs (HeNBs), within the coverage area of macrocells the dense deployment reduces the distance between base stations and users, thereby decreasing path loss and allowing frequencies to be reused at more locations. This results in a significant increase in network capacity [2], [4].

However, these UDN advantages are accompanied by new challenges. The dense deployment of small cells with limited frequency resources inevitably leads to complex interference issues [5], [6]. Although UDNs promise substantial capacity enhancement, this is constrained by co- tier interference from adjacent femtocells along with cross-tier interference between macrocells and femtocells sharing a single channel, where each contributes to a decline in the received signal quality [7], [8].

In addition to UDN, Reconfigurable Intelligent Surfaces (RIS) are increasingly regarded as an effective technology for increasing signal quality in wireless communications [9]. RIS consist of many passive reflector elements, each of which can be phase-tuned to be directed toward the receiver in a focused manner so that the reflected signals reinforce one another. [10]. Thus, RIS is capable of improving the quality of the received signal, making it suitable for UDNs where femtocell transmission power is limited [11]. However, in signal reflection, these elements lack selectivity, so that interference signals are also reflected toward the receiver, making interference more complex with the implementation of RIS in a UDN environment. Therefore, interference management is required to handle interference resulting from dense femtocell deployment as well as additional interference from RIS reflections, so that both technologies can operate optimally.

The interference management techniques to be discussed are clustering and Soft Fractional Frequency Reuse (FFR). The clustering method groups femtocells that are in close proximity to one another; then, femtocells within a single group are assigned different co-channel allocations to minimize the occurrence of co-channel interference [12]. Clustering can be performed statically or adaptively. Static clustering performs grouping and co-channel allocation at the beginning and does not change, so it cannot adapt when network conditions change. Conversely, Dynamic Clustering can dynamically update cluster formation and channel allocation based on current interference conditions [13]. Thus, Dynamic Clustering is superior because it maintains signal quality in dynamic networks and is particularly effective at mitigating co-tier interference [14]. On the other hand, Soft-FFR can handle cross-tier interference, which occurs between macrocells and femtocells. Soft-FFR divides the macrocells coverage service area into two zones, referred to as the central zone and the edge zone with different transmit power settings and frequency allocations in each zone. Users in the edge zone, who are more susceptible to interference, are given stricter co-channel allocation, while users in the central zone have more flexibility in using co-channel allocation. This reduces signal overlap [15]. Thus, Soft-FFR complements the clustering capability in handling co-tier and cross-tier interference in RIS-assisted UDNs

Several studies have examined RIS-assisted UDNs from various perspectives. Lin and Yu [16] investigated the performance of RIS-assisted UDNs by employing a ternary stochastic geometry approach. The results showed that the presence of RIS improves system performance, particularly for users with high SINR. Huang et al. [17] optimized the RIS reflector configuration for energy efficiency, enabling RIS to provide higher energy efficiency compared to conventional amplifier systems. To address interference through clustering, Farhan and Rizvi [18] formed clusters in a three-layer heterogeneous network and managed inter-cluster channel allocation, thereby increasing system throughput and reducing interference between small cells. Soleimani and Sabbaghian [19] clustered femto access points and femto users according to the best line-of-sight connectivity; this approach lowered co-channel interference and increased the achievable data rate. Several works also discuss the use of FFR to address cross-tier interference. Novlan et al. [20] analytically evaluated FFR in an OFDMA network and found improved SINR and data rates at the cell edge, while Alotaibi [21] implemented dynamic FFR in a 5G network, resulting in reduced interference between macrocells and femtocells and increased network capacity.

Table 1 positions these studies with respect to the interference components they address, whether the reflective behaviour of a RIS is taken into account, and whether the allocation adapts to the network state.

Table 1: Positioning of the proposed scheme with respect to related work

Study	Co-tier	Cross-tier	RIS-aware	Adaptive
Lin and Yu [16]	No	No	Yes	No
Huang et al. [17]	No	No	Yes	No
Farhan and Rizvi [18]	Yes	No	No	No
Soleimani and Sabbaghian [19]	Yes	No	No	No
Novlan et al. [20]	No	Yes	No	No
Alotaibi [21]	No	Yes	No	Yes
Bai et al. [22]	Yes	No	No	Yes
Proposed scheme	Yes	Yes	Yes	Yes

The existing literature indicates that the integration of Dynamic Clustering and soft-FFR in RIS-assisted UDN for the simultaneous mitigation of co-tier and cross-tier interference has not been comprehensively investigated. Most studies focus only on one component of interference, without adaptively integrating both. To address this gap, this study proposes an adaptive interference management scheme that integrates Dynamic Clustering with Soft-FFR in RIS-assisted UDNs.

The contribution of this work is therefore not the empirical pairing of two established techniques, but an analysis of how a passive RIS scales the interference of an ultra-dense network, together with the interference management scheme that this analysis motivates. Three points are claimed. First, in Section 2.6 the RIS array gain of (1) is substituted into the interference terms of (2), which shows that the same factor $(N+1)^2$ multiplies the desired and the co-channel components. The attainable SINR therefore saturates at a ceiling that is fixed by the reflected interference and is independent of the number of reflecting elements, so that enlarging the surface cannot by itself improve the SINR of an interference-limited UDN. Because the reflected interference carries a co-tier and a cross-tier contribution, this ceiling can be raised only if both are reduced, and the joint use of clustering and Soft-FFR therefore follows from the model rather than being assumed. Second, we introduce the vulnerability weight in (10), which makes the cluster-formation order an explicit function of the Soft-FFR zone label in (11) and of the normalised SINR deficit with respect to the threshold, and we state it as a greedy priority rule for the underlying channel-assignment objective. By construction the two mechanisms then operate on a shared state variable rather than being applied one after the other, which is the structural difference between the proposed scheme and a sequential combination of [21],[22]. Third, the periodic re-clustering used in earlier dynamic schemes is replaced by an event-triggered rule, so that the number of adaptation events follows the number of SINR threshold violations rather than the length of the observation window; the resulting behaviour is characterised in Section 2.6.

This paper proposes adaptive interference management using an Dynamic Clustering approach that groups nearby femtocells and assigns different co-channels to each cluster member, which can be adjusted according to network conditions to mitigate co-tier interference, while FFR divides the macrocells area into central and peripheral zones with tiered power levels to mitigate cross-tier interference. The integration of these approaches is intended to simultaneously suppress both co-tier and cross-tier interference, thereby enhancing the performance of RIS-assisted UDNs. System performance is evaluated in terms of SINR, throughput, and BER.

2. System Model

This study aims to mitigate interference in UDN environments. The analysis is conducted on cellular networks utilizing OFDMA-based downlink communication. Four simulation scenarios are proposed and evaluated sequentially as follows: (1) the baseline system, (2) the Dynamic Clustering System, (3) the Dynamic Soft-FFR System, and (4) the proposed system that adaptively integrates clustering and Soft-FFR. The four scenarios are evaluated under the same network topology, in which three macrocells are deployed using a frequency reuse factor (FRF) of 3; as a result, each macrocell occupies one-third of the total system bandwidth. In every macrocell, femtocells are distributed in a dense and uniform manner, and the FRF scheme together with their locations determines the random allocation of one-third of the available bandwidth to each of them. All femtocells are assumed to actively transmit data from the Home eNodeB (HeNB) to the Femtocell User Equipment (FUE). To enhance signal quality, a RIS is positioned at the intersection center of the three macrocells, enabling directional reflection of wireless signals.

2.1 Baseline System

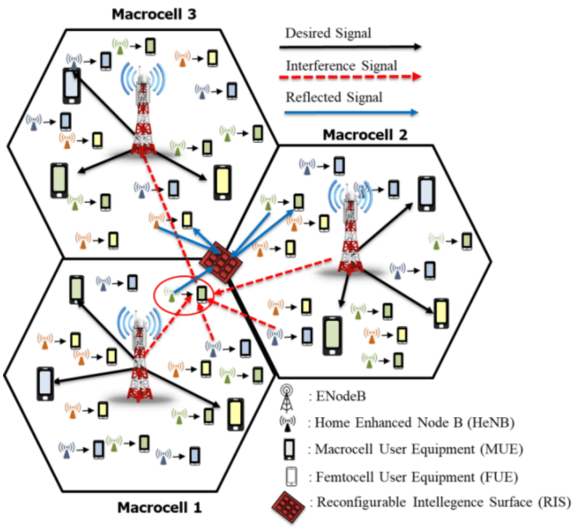

Figure 1: Baseline System Scenario (RIS-Assisted UDN)

Based on the configuration shown in Figure 1, the analyzed femtocell network experiences both co-tier and cross-tier interference. To manage spectrum resources, different sub-bandwidth allocations are applied to macrocells and femtocells using the FRF scheme. The macrocell operates with an FRF of 1, while the femtocells employ an FRF of 3. Accordingly, the overall system bandwidth is divided into three identical channels, namely Channel 1, Channel 2, and Channel 3, which are assigned cyclically to femtocells according to their positions within the macrocell coverage region. This condition increases the occurrence of interference between femtocells, especially at high femtocell densities. Cross-tier interference results from interference from neighboring macrocells as well as signal reflections through the RIS. Model 1 is configured without interference management to serve as a baseline for the next three models.

2.2 Dynamic Clustering System

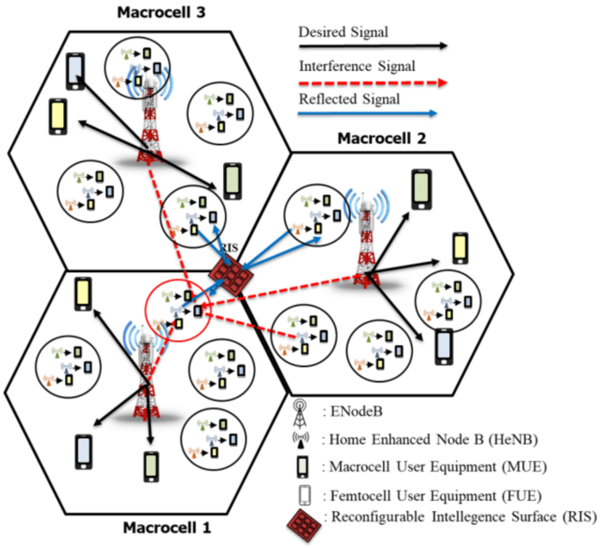

Figure 2: Clustering System

The second scenario modifies the baseline by forming clusters of three adjacent femtocells; following the FRF-3 scheme, every femtocell belonging to a cluster is then allocated a different channel. Cluster formation begins by selecting the femtocell with the shortest distance to the eNodeB as the reference femtocell; next, the two femtocells closest to the reference are selected to complete the first cluster. Once formed, the procedure is repeated until all femtocells in the macrocellsarea have formed clusters.

This method aims to increase the distance so that the co-tier interference received by each femtocell decreases. This dynamic nature arises from periodic cluster updates as network conditions change; for example, when the estimated SINR of a number of HeNBs decreases, the clustering process is rerun, prioritizing HeNBs with low SINR values so that the cluster configuration always adapts to current conditions.

2.3 Dynamic Soft-FFR System

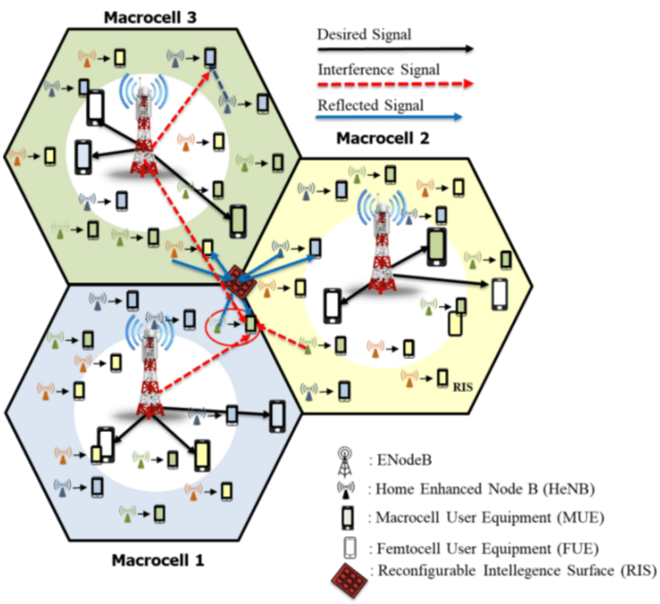

Figure 3: FFR System

The third scenario divides each macrocells into a center zone and an edge zone based on the FUE distance to the eNodeB, with the boundary set at half the macrocells radius. In the center zone, all neighboring macrocells are counted as cross-tier interferers, and co-tier interference is calculated in full, as in the baseline. In the edge zone, FRF 3 is applied so that only macrocells using the same channel interfere, and co-tier interference is reduced by 25% to account for the elimination of a quarter of the subchannels. HeNBs in the edge zone select channels based on their distance from the ENodeB. With this configuration, the third model is optimized to improve user service quality in the edge zone, which is most vulnerable to interference. The term "dynamic" refers to the determination of zones and the relocation of edge channels, which are recalculated based on the user's position and conditions at each evaluation, rather than being set once at the beginning.

2.4 Proposed System

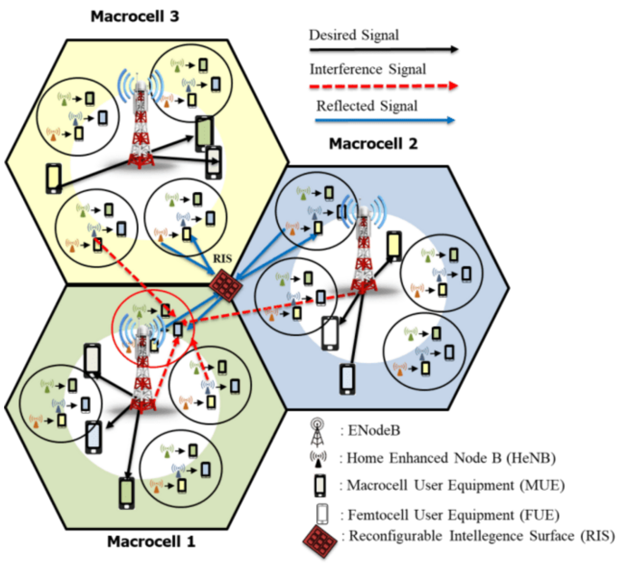

Figure 4: Proposed System

The fourth scenario integrates the second and third scenarios into a single adaptive framework. The approach involves assigning complementary roles to the two models: Soft-FFR addresses cross-tier interference through zone partitioning, while clustering addresses co-tier interference through channel separation between femtocells. To achieve an adaptive configuration in this method, reclustering is not performed uniformly but is triggered by network conditions and directed to protect vulnerable HeNBs. Reclustering is performed if there is a HeNB with an estimated SINR value below the threshold. Each HeNB is assigned a priority weight according to its level of vulnerability to interference, so that limited channel resources are prioritized to maintain the HeNBs that need it most. Meanwhile, cross-tier interference follows the Soft-FFR rules, while co-tier interference follows the channel separation results from clustering; specifically, in the edge zone, an additional 25% reduction is applied in accordance with the elimination of co-channel subchannels. The total interference for each FUE also accounts for the reflection component from the RIS. In a single cycle, this proposed model encompasses several stages, including femtocell deployment, zone formation, SINR threshold calculation, evaluation of reclustering trigger conditions, weighted cluster formation, channel allocation, per-zone interference calculation, and SINR evaluation.

2.5 Performance Metrics

The analysis of the RIS-based communication system in this work adopts the two-ray channel model described in [23]. Based on this configuration, Equation (1) is used to calculate the received signal power

$$P_r = (N + 1)^2 . P_t . (\frac{\lambda}{4\pi d})^2 \quad (1)$$

Interference occurs when femtocells using identical frequency channel allocations transmit downlink signals simultaneously. In such cases, the Signal-to-Interference-plus-Noise Ratio (SINR) is calculated using Equation (2)

$$SINR_{femto} = \frac{P_{femto}}{\sum_{i=1}^{x} I(i) + \sum_{j=1}^{y} I(j) + P_N} \quad (2)$$

where $P_{\_femto}$ is received the signal power of the target femtocell in mW or W. The paramaters x and y indicate the number of co-channel interfering HeNBs and eNodeBs, respectively. . $I(j)$ and $I(i)$ denote the interference powers generated by the j-th HeNB and the i-th eNodeB operating on a shared frequency resource, while P_N refers to the receiver noise power.

The estimated signal strength in FUE, measured in decibels (dB), can be determined using the following Equation (3)

$$P_{\_FUE}(dBm) = P_{\_HeNB}\,(dBm) - L\,(dB) \quad (3)$$

In that Equation $P_{\_HeNB}$ is the HeNB transmit power in dBm, and L is the path loss in dB. Since the network is assumed to operate in an urban environment, the macrocells and femtocell channel models refer to 3GPP TR 36.922 version 10.0.0 Release 10 and 3GPP TR 36.814 version 10.2.0 [23]. The path loss equation for macrocells and femtocells are shown in Equation (4) and (5).

$$L_{\_macro}(dB) = 15.3 + 37.6\, log_{10}(r) + L_{\_oth} \quad (4)$$

$$L_{\_Femto}(dB) = 127 + 30\, log_{10}\,(\frac{r}{1000}) \quad (5)$$

where r indicates the separation between the transmitting and receiving nodes, measured in meters, while $L_{\_oth}$ is the additional propagation loss expressed in dB.

The thermal noise power P_N in Equation (2) is calculated from the spectral noise power density N_0, the bandwidth B (in Hz), and the noise figure of the receiver, as shown in Equation (6)

$$P_N = N_0 + 10\log_{10}(B) + N \quad (6)$$

The Cumulative Distribution Function (CDF) characterizes the cumulative probability of a continuous random variable. In this study, the CDF of the SINR is determined according to Equation (7)

$$P_{\_OUT}\,(SINR \le r) = P[SINR \le r] \quad (7)$$

where r represents the SINR value under analysis, which is assumed to remain constant throughout the evaluation.

Throughput refers to the total number of bits successfully received by the destination per unit time, serving as a key indicator of system capacity. This value is calculated based on Shannon's capacity equation shown in Equation (8).

$$T = \text{B} \times \log_2(1 + \text{SINR}) \quad (8)$$

where T i is the throughput attained by the system, expressed in Mbps, while (B) denotes the total bandwidth allocated to the system in MHz.

The BER (Bit Error Rate) denotes the proportion of bits received incorrectly in a communication system due to the effects of noise, interference, or synchronization errors. In this study, the BER values for the 16-QAM modulation in the observed FUE were calculated using the following Equation(9)

$$BER = \frac{3}{4} Q\left(\sqrt{\frac{4}{5} \times \frac{E_b}{N_O}}\right) \quad (9)$$

where $Q(x)$ refers to the Q-function used in error probability analysisE_b is the energy per transmitted bit, and N_O denotes the noise power spectral density. The E_b/N_O ratio is determined based on the modulation scheme utilized by the communication system.

Each HeNB is assigned a priority weight w_f, the value of which increases when its estimated SINR falls below the threshold γ_{th} or when it is in the edge zone, as shown in Equation (10). The notation $(x)^+$ denotes max (x, 0) and κ is a weighting constant.

$$w_f = \frac{(\gamma_{th} - \gamma(f))^+}{\gamma_{th}} + \kappa \cdot \mathbf{1}\{zone(f) = EDGE\} \quad (10)$$

The adaptive mechanism in the proposed model is implemented by defining a soft-FFR zone for each FUE based on its distance from the ENodeB, as given in the Equation(11).

$$zone(u) = \begin{cases} EDGE, & d(u, eNB) \geq R/2 \\ CENTER, & d(u, eNB) < R/2 \end{cases} \quad (11)$$

2.6 Interference Scaling in RIS-Assisted UDN, Computational Complexity, and Signaling Overhead

The received power model in (1) applies an array gain of $(N+1)^2$ to any signal that reaches the receiver through the surface, in line with the quadratic power scaling reported for passive reflecting surfaces [10],[24],[25]. Because the elements are passive and share a single phase configuration, this gain is not selective: a co-channel signal whose path traverses the surface is reinforced by the same factor as the desired signal. Consistent with the reflection model adopted in (1), the surface is therefore assumed to apply its array gain to every co-channel path that traverses it, which represents the worst case for a passive surface whose phase configuration is not user-selective. Separating the interference of (2) into a reflected component and a direct component then gives Equation (12).

$$\text{SINR\_f} = \frac{(N+1)^2 \text{ P\_d,f}}{(N+1)^2 \text{ I\_RIS,f} + \text{I\_dir,f} + \text{P\_N}} \quad (12)$$

where P_d,f is the desired power received from the serving HeNB, I_RIS,f the co-channel interference whose path traverses the surface, and I_dir,f the co-channel interference reaching the FUE directly. For N = 0 the expression reduces to the conventional interference-limited SINR of (2), whereas for large N the factor $(N+1)^2$ cancels between the numerator and the leading term of the denominator, which gives the far-field asymptote of Equation (13) [23].

$$\lim_{n \to \infty} \text{SINR\_f} = \frac{\text{P\_d,f}}{\text{I\_RIS,f}} \quad (13)$$

The attainable SINR is therefore bounded by a ceiling that depends only on the reflected co-channel interference and is independent of N: once I_RIS,f dominates I_dir,f and the noise, which is the regime of a UDN at high femtocell density, enlarging the surface brings no further gain, and the ceiling can be raised only by reducing the number of interferers whose paths traverse it. A comparable saturation has been reported for RIS-assisted links limited by electromagnetic interference [25], although there the ceiling arises from interference impinging on the surface rather than reflected by it. Since I_RIS,f carries both a co-tier and a cross-tier contribution, clustering and Soft-FFR must act together rather than alternatively, so that the joint scheme of Section 2.4 follows from (13) rather than being assumed. Because an exact assignment of K = 3 orthogonal channels is combinatorial and intractable at these densities, (10) is used as a greedy priority rule: it orders the HeNBs by normalised SINR deficit and promotes those in the edge zone, so that the zone label of (11) and the deficit enter a single ordering and the two mechanisms act on a shared state variable rather than in sequence. Re-clustering is triggered only when a HeNB falls below the threshold.

The per-cycle cost is dominated by cluster formation, which selects a reference HeNB together with its two nearest neighbour M/K times and is $O(M^2)$; zone assignment, weighting and channel allocation are of lower order. The scheme is therefore of the same complexity as the conventional Dynamic Clustering of Section 2.2, or about 5×10^4 distance evaluations per cycle for the M = 330 of Section 3. Each cycle exchanges 2M control messages, that is 660 per macrocell.

3. Results and discussion

The simulation was conducted on a multi-cell network consisting of three macrocells with a FRF of 3. Each macrocells has a radius of 1000 m, while the femtocell radius is set at 30 m. A total of 330 femtocells were randomly distributed according to a uniform distribution across the area of the each macrocells to form a UDN environment. The femtocells also employ an FRF of 3 and serve a single FUE located at a fixed distance of 10 m from the HeNB. The maximum transmit power levels assigned to the eNB and HeNB are 46 dBm and 23 dBm, respectively. In addition, the network is configured with a total bandwidth of 10 MHz and a 16-QAM modulation format. The simulation was conducted using MATLAB and run for 10,000 iterations. In each iteration, performance parameters such as SINR, throughput, and BER were calculated, and their average values were used for system performance analysis. Additionally, the distributions of SINR and throughput were evaluated using the CDF and the distributions of BER were evaluated using the CCDF. Table 2 gives an overview of the parameters used in the simulations conducted in this study.

Table 2: Simulation Setup Parameters

No.	Parameter	Value
1.	Macrocells	3
2.	HeNBs (in each macrocell)	330
3.	FUEs (in each macrocell)	330
4	Femtocell Radius	30 m
5.	Macrocell Radius	1,000 m
6.	FRF of macrocells and femtocells	1 and 3
7.	System Bandwidth	10 MHz
8.	HeNB TransmitPower	23 dBm
9.	eNodeB TransmitPower	46 dBm
10.	Modulation scheme	16-QAM
11.	Noise Power Spectral Density	-174 dBm/Hz
12.	Iterations	10,000 iterations

To evaluate the performance of the four systems considered, a thorough set of simulations was performed. The first configuration, illustrated in Figure 1, represents the baseline UDN network assisted by RIS and is denoted by the blue trendline. The second configuration, referred to as **Dynamic Clustering**, implements the clustering mechanism presented in Figure 2 and is represented by the green trendline. The third configuration, termed **Dynamic Soft-FFR**, incorporates the Dynamic Soft-FFRscheme described in Figure 3 and is indicated by the red trendline. Finally, the proposed integrated method combines RIS-assisted UDN, Dynamic Clustering, and Dynamic Soft-FFR into a unified framework. The performance of this integrated system is represented by the purple trendline. All four configurations were evaluated under the same topology, transmit powers, bandwidth, channel models and number of iterations, so that the differences reported below are attributable to the interference management mechanism alone rather than to differing simulation assumptions.

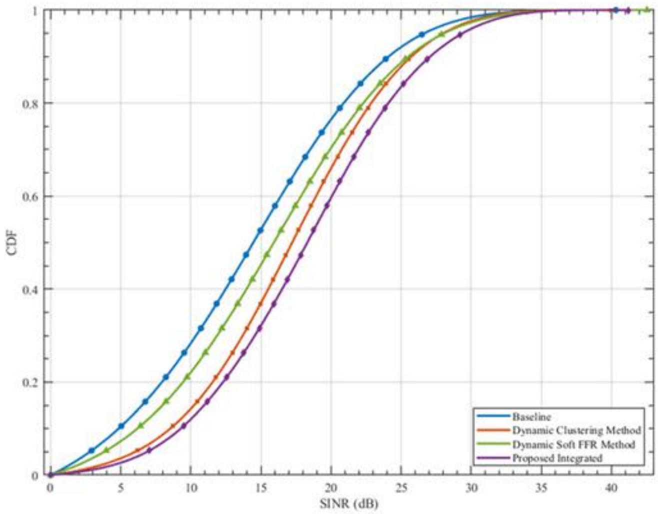

Figure 5: The CDF of SINR

As shown in Figure 5 presents the CDF of the SINR. Because the CDF expresses the probability that a user experiences an SINR lower than or equal to a given value, a curve positioned further to the right (a lower CDF at a fixed SINR) indicates that a larger share of users obtains a high SINR, which is desirable. At the reference level of 20 dB, the baseline records a CDF of about 64%, meaning that roughly two-thirds of users fall below 20 dB. This value decreases to approximately 53% for Dynamic Soft-FFR and 47% for Dynamic Clustering, while the proposed scheme attains the lowest value of about 43%.

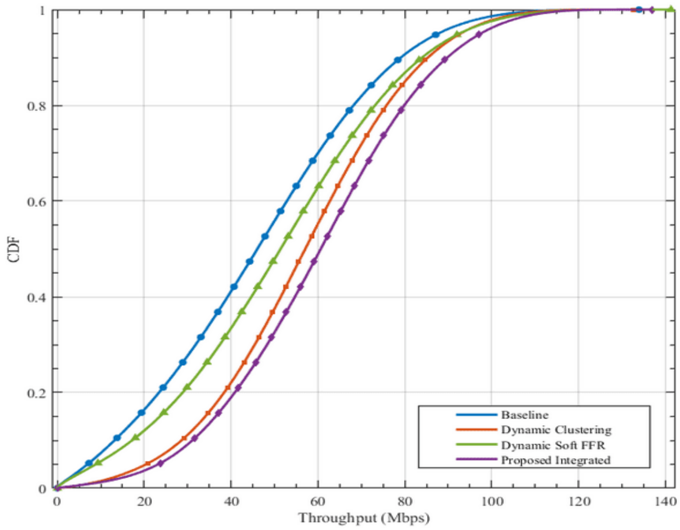

Figure 6: The CDF of throughput

JTEIN: Jurnal Teknik Elektro Indonesia, Vol. 7, No. 2, pp. 206-219, 2026
e-ISSN 2723-0589

As depicted in Figure 6, the CDF of the throughput, which follows the same interpretation: a lower CDF at a given throughput indicates that more users reach that data rate. At a reference throughput of 70 Mbps, the baseline records a CDF of about 84%, whereas Dynamic Soft-FFR, Dynamic Clustering, and the proposed scheme record approximately 75%, 68%, and 62%, respectively. The proposed method therefore leaves only about 62% of users below 70 Mbps, corresponding to a reduction of roughly 22 percentage points relative to the baseline.

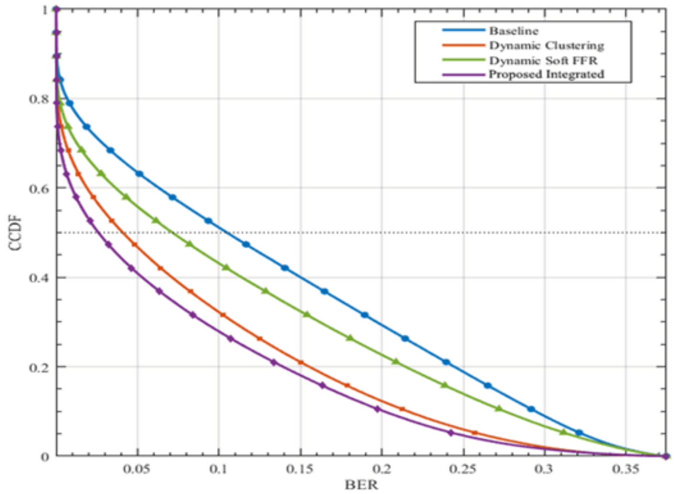

Figure 7: The CCDF of BER

Figure 7 depicts the CCDF of the BER for the 16-QAM modulation. At a CCDF of 0.5, the proposed scheme yields a BER of about 0.05, compared with approximately 0.07 for Dynamic Clustering, 0.10 for Dynamic Soft-FFR, and 0.13 for the baseline. The proposed method therefore reduces the BER by roughly 60% relative to the baseline, indicating markedly more reliable bit-level transmission. A notable observation is that Dynamic Clustering achieves a lower BER than Dynamic Soft-FFR, even though their SINR and throughput distributions are comparable. This suggests that, at the FUE located close to its serving HeNB, the dominant source of bit errors is the co-tier interference generated by the densely packed neighbouring femtocells rather than the cross-tier interference from the macrocells. Channel separation through clustering attacks this dominant component directly and therefore has a stronger effect on the error floor. The proposed scheme retains the clustering benefit while adding the zone-based cross-tier mitigation of Soft-FFR, which is why it attains the lowest BER among all configurations and offers the best communication reliability

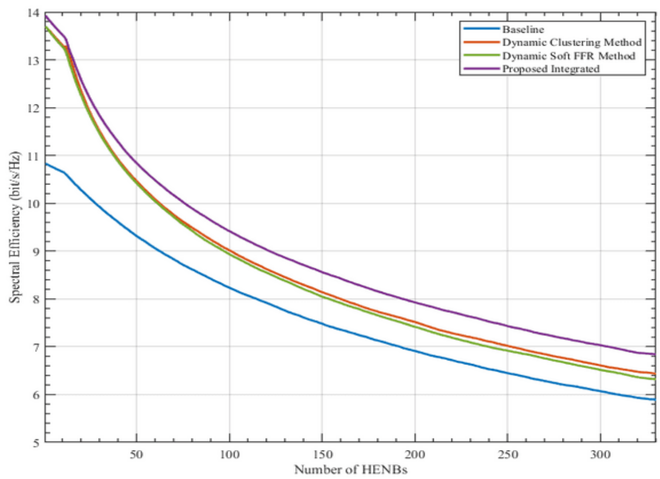

Figure 8: The results of Spectral efficiency

Figure 8 presents the spectral efficiency as the number of HeNBs increases. A general downward trend is observed for all schemes, because a denser deployment intensifies the aggregate interference and erodes the achievable efficiency. At the maximum density of 330 HeNBs, the baseline achieves about 5.9 bit/s/Hz, while Dynamic Soft-FFR, Dynamic Clustering, and the proposed scheme reach approximately 6.4, 6.5, and 6.9 bit/s/Hz, respectively. Although every scheme degrades as the network becomes denser, the proposed method consistently sustains the highest spectral efficiency and exhibits the gentlest decline, indicating that its adaptive interference management remains effective even under heavy load. The gain of about 1.0 bit/s/Hz over the baseline at maximum density (roughly a 17% improvement) demonstrates that combining clustering with Soft-FFR allocates the available frequency resources more efficiently, so that the spectrum continues to be exploited productively as the network scales.

The comparisons above are supported by the sampling statistics of the simulation output. Each metric is estimated from the 10,000 independent simulation runs listed in Table 2. Within a run, the per-user values are averaged first, since users in the same run share a topology and are therefore not independent; the mean and its 95% confidence interval are then computed across the 10,000 run averages and reported in Table 3.

Table 3: Mean performance with 95% confidence intervals

Scheme	SINR (dB)	Throughput (Mbps)	BER
Baseline	13.06 ± 0.01	46.41 ± 0.04	0.1263 ± 0.0002
Dynamic Soft-FFR	14.69 ± 0.01	51.27 ± 0.04	0.1062 ± 0.0002
Dynamic Clustering	16.85 ± 0.01	57.02 ± 0.03	0.0771 ± 0.0001
Proposed	17.91 ± 0.01	60.43 ± 0.03	0.0670 ± 0.0001

Pairwise comparisons using a two-sample Welch t-test on the means and a two-sample Kolmogorov–Smirnov test on the distributions return $p < 0.001$ for every metric and every pairing. The narrowest margin is the one over the clustering configuration, namely 1.06 dB in SINR, 3.40 Mbps in throughput and 0.0100 in bit error rate; the margins over the frequency-reuse configuration and the baseline are larger, as Table 3 shows. Because the number of replications is large, it is the magnitude of each margin rather than its statistical significance that should be read as the practical result.

Since the Dynamic Clustering and Dynamic Soft-FFR configurations implement clustering [13] and fractional frequency reuse [21] under the same topology, transmit powers, bandwidth, channel models and number of iterations, the results above quantify the gain of the proposed scheme over these established approaches and not over the unmanaged baseline alone. Relative to the clustering configuration, the CDF of the SINR at 20 dB falls from about 47% to 43%, that of the throughput at 70 Mbps from 68% to 62%, the BER at a CCDF of 0.5 from 0.07 to 0.05, and the spectral efficiency at 330 HeNBs rises from 6.5 to 6.9 bit/s/Hz; the gains over the frequency-reuse configuration are larger still.

That the clustering margin is the narrower of the two follows from Section 2.6: at an FUE close to its serving HeNB the co-tier term dominates the reflected interference, so a scheme that already separates co-channel HeNBs recovers most of the available gain, and the remainder comes from the zone-based mitigation of the cross-tier component. Both approaches were re-evaluated here under a common set of assumptions rather than compared through the values reported in their original studies, which assume different cell radii, femtocell densities and propagation models and include no reflecting surface

4. Conclusion

This study evaluated four RIS-assisted UDN configurations, namely a baseline system and three adaptive interference management techniques: Dynamic Clustering, Dynamic

Soft-FFR, and a proposed scheme that adaptively integrates clustering with Soft-FFR. The simulations, carried out on a three-macrocell network with 330 femtocells per macrocell over 10,000 iterations, consistently show that the proposed method delivers the best overall performance among the considered systems.

At an SINR of 20 dB, the CDF decreases from about 64% for the baseline to 53% for Dynamic Soft-FFR, 47% for Dynamic Clustering, and 43% for the proposed scheme, meaning that more users achieve a high SINR. The same trend holds for throughput, where the CDF at 70 Mbps falls from about 84% to 62%, and for spectral efficiency at 330 HeNBs, which rises from about 5.9 to 6.9 bit/s/Hz. The proposed method also attains the lowest bit error rate, approximately 0.05 against 0.13 for the baseline, confirming that it provides more reliable communication.

These findings demonstrate that Dynamic Clustering and Dynamic Soft-FFR play complementary roles in suppressing co-tier and cross-tier interference, respectively, and that integrating them within an adaptive, vulnerability-aware framework yields the most robust improvement in service quality for dense RIS-assisted UDNs. Future work may extend the scheme by jointly optimising the RIS phase configuration with the clustering and zone-allocation decisions, and by validating the approach under user mobility and more diverse traffic conditions. A further limitation of the present study is that the comparison is restricted to schemes in which the RIS phase configuration is fixed; benchmarking against optimisation- or learning-based RIS configuration methods requires a system model in which the phase configuration is itself a decision variable, and is left to future work

References

[1] A. A. Basahel, M. R. Islam, and M. H. Habaebi, “6G networks: insights and reliability analysis,” *Bull. Electr. Eng. Informatics*, vol. 13, no. 6, pp. 4048–4057, 2024.

[2] Y. Li, C. Yin, T. Do-Duy, A. Masaracchia, and T. Duong, “Aerial Reconfigurable Intelligent Surface-enabled URLLC UAV Systems,” *IEEE Access*, vol. PP, p. 1, 2021, doi: 10.1109/access.2021.3119268.

[3] S. J. Kim and J. G. Kim, “Resource Allocation in Cluster Based Ultra Dense Network,” in *Proc. Int. Conf. ICT Convergence (ICTC)*, Jeju, 2020, pp. 1128–1131.

[4] O. Ansari and H. Guo, “Extending Near Field Communication Range for Ultra-Dense Internet of Things,” *EEE J. Radio Freq. Identif*, vol. 8, pp. 770–779, 2024.

[5] G. V. Adekogba, K. B. Adedeji, and Y. O. Olasoji, “Interference Reduction Scheme for Femtocell Ultra-Dense-Network: Concept and Research Challenges,” *ITEGAM-JETIA*, vol. 10, no. 49, pp. 144–158, 2024.

[6] S. Suryani, M. Susanto, A. Sadnowo, and S. N. Hasim, “Interference Management Using Power Allocation for Downlink Transmission of Femtocell-Macrocell Ultra Dense Networks,” in *Proc. 9th ICITACEE*, Semarang, 2022, pp. 184–188.

[7] M. Susanto, A. G. Gumilang, H. Fitriawan, and A. A. Aziz, “Interference management based on clustering in RIS-aided ultra dense network under multicell scenario,” *Bull. Electr. Eng. Informatics*, 2025, doi: 10.11591/eei.v14i4.9495.

[8] A. G. Gumilang, M. Susanto, and H. Fitriawan, “Interference Management Based on Clustering Method for Ultra-Dense Networks in Multicellular Network,” *J. Tek. Elektro*, 2023, doi: 10.15294/jte.v15i2.48738.

[9] S. et al Hassouna, “A survey on reconfigurable intelligent surfaces: Wireless communication perspective,” *IET Commun.*, vol. 17, no. 5, pp. 497–537, 2023.

[10] Q. Wu and R. Zhang, “Intelligent Reflecting Surface Enhanced Wireless Network via Joint Active and Passive Beamforming,” *IEEE Trans. Wirel. Commun.*, vol. 18, no. 11, pp. 5394–5409, 2019, doi: 10.1109/TWC.2019.2936025.

[11] H. et al Yang, “Beyond Limitations of 5G with RIS: Field Trial in a Commercial

Network, Recent Advances, and Future Directions," *IEEE Commun. Mag.*, vol. 62, no. 11, pp. 132–138, 2024.

[12] T. T. Bui, L. D. Nguyen, H. H. Kha, and T. Q. Duong, "Joint Clustering and Resource Allocation Optimization in Ultra-Dense Networks with Multiple Drones as Small Cells Using Game Theory," *Sensors*, vol. 23, no. 8, 2023.

[13] W. Bai, Y. Li, T. Yao, and H. Zhang, "Performance Analysis of Dynamic Re-Clustering and Resource Allocation in Ultra Dense Network," *IEEE Access*, vol. 6, pp. 60891–60899, 2018, doi: 10.1109/ACCESS.2018.2870868.

[14] S.-J. Kim and J.-G. Kim, "Location-Based Resource Allocation in Ultra-Dense Network with Clustering," *Sensors*, vol. 21, no. 12, 2021.

[15] P. Yen, Q. Zhan, and H. Minn, "New fractional frequency reuse patterns for multi-cell systems in time-varying channels," *IEEE Wirel. Commun. Lett.*, vol. 4, no. 3, pp. 253–256, 2015, doi: 10.1109/LWC.2015.2404787.

[16] H.-C. Lin and Q.-Y. Yu, "Ternary Stochastic Geometry Theory for Performance Analysis of RIS-Assisted UDN," *IEEE Trans. Commun.*, vol. 73, no. 1, pp. 600–613, 2025.

[17] C. Huang, A. Zappone, G. C. Alexandropoulos, M. Debbah, and C. Yuen, "Reconfigurable Intelligent Surfaces for Energy Efficiency in Wireless Communication," *IEEE Trans. Wirel. Commun*, vol. 18, no. 8, pp. 4157–4170, 2019.

[18] N. Farhan and S. Rizvi, "An Interference-Managed Hybrid Clustering Algorithm to Improve System Throughput," *Sensors (Basel).*, vol. 22, 2022, doi: 10.3390/s22041598.

[19] B. Soleimani and M. Sabbaghian, "Cluster-Based Resource Allocation and User Association in mmWave Femtocell Networks," *IEEE Trans. Commun.*, vol. 68, no. 3, pp. 1746–1759, 2020.

[20] T. D. Novlan, R. K. Ganti, A. Ghosh, and J. G. Andrews, "Analytical Evaluation of Fractional Frequency Reuse for OFDMA Cellular Networks," *IEEE Trans. Wirel. Commun*, vol. 10, no. 12, pp. 4294–4305, 2011.

[21] S. Alotaibi, "Network Capacity Improvement in 5G by Using Dynamic Fractional Frequency Reuse," *J. Umm Al-Qura Univ. Eng. Archit.*, vol. 14, pp. 105–114, 2023.

[22] W. Bai, Y. Li, T. Yao, and H. Zhang, "Performance Analysis of Dynamic Re-Clustering and Resource Allocation in Ultra Dense Network," *IEEE Access*, vol. 6, pp. 60891–60899, 2018.

[23] 3GPP (3rd Generation Partnership Project), "TR 36.814 V10.2.0 / TR 36.922 V10.0.0."

[24] E. Bjornson and L. Sanguinetti, "Power Scaling Laws and Near-Field Behaviors of Massive MIMO and Intelligent Reflecting Surfaces," *IEEE Open J. Commun. Soc.*, vol. 1, no. August, pp. 1306–1324, 2020, doi: 10.1109/OJCOMS.2020.3020925.

[25] Ö. Ö. and E. G. L. E. Björnson, "Intelligent Reflecting Surface Versus Decode-and-Forward: How Large Surfaces are Needed to Beat Relaying?," *IEEE Wirel. Commun. Lett.*, vol. 9, no. 2, pp. 244–248, 2020.